PEGASUS – a review of in-orbit operation and obtained results

C. Scharlemann, B. Seifert, R. Schnitzer, R. Kralofsky, C. Obertscheider
University of Applied Sciences Wiener Neustadt, FOTEC GmbH, Wiener Neustadt

M. Taraba[1,2], T. Dorn[2], T. Turetschek[2], H. Fauland[2], R. Plötzeneder[2], R. Stockinger[2]
(1) University of Vienna, Faculty of Physics, (2) Space Tech Group Austria, STG-A

M. Schmid
University of Vienna, Department of Astrophysics

T. Riel, A. Sinn, G. Janisch, F. Deisl, D. Kohl
TU of Vienna, Space Team

B. Lybekk, H. Hoang, E. Trondsen
University of Oslo, Department of Physics

Abstract:

The QB50 project is an international project with the goal of sending an extended number of nanosatellites, a.k.a. CubeSats, into the Thermosphere. The scientific goal of this mission is to monitor over a period of up to nine months the prevailing conditions in this rather unknown part of Earth's atmosphere. Each of the CubeSats will be equipped with one of three possible scientific instruments: (i) a set of Langmuir probes, (ii) atomic oxygen measurement device, (iii) ion/neutral mass spectrometer.

In 2017, 36 nanosatellites were launched in the framework of QB50. The first batch included 28 CubeSats deployed from the ISS in April 2017, followed by a second batch of eight satellites two months later on the 23rd of June by means of the Indian launcher PSLV. One of the eight satellites from the second batch was the Austrian CubeSat PEGASUS.

PEGASUS is equipped with the Langmuir probe instrument from the University of Oslo. Beside of its scientific mission, the satellite serves as a test bed for several subsystems which were developed by the PEGASUS team including

- A TT&C board with two redundant transceivers and corresponding controllers combined on one board. Both transceiver-controllers can be operated independently in the same or different frequencies, with the same or different RX or TX frequencies.
- Multifunctional structure elements: beside of its mechanical tasks, the structural elements of PEGASUS serve also as a bus system, house the magnetotorquers for the ADCS and serve as solar cell array. This allows a very compact design and avoids (nearly) completely the use of cables inside the satellite.

In addition to the in-space technology, also a ground station network and a dedicated PEGASUS datacenter has been developed. The ground stations (in total four ground stations distributed in Austria) are interconnected but can operate independent from each other to ensure uninterrupted operation of at least 1 ground station at any time during the mission. All data received by any of the four ground stations are send to and collected by a dedicated data server. This server features also an interface for radio amateurs who can upload beacons and data they managed to receive.

PEGASUS has performed very well since in orbit and the PEGASUS team was able to download a large amount of house-keeping data, as well as scientific data. The present paper provides a summary of the in-orbit measurement and the lessons learned.

NOMENCLATURE:

ADC	Analog to digital converter
ADCS	Attitude Determination and Control System
AX.25	Amateur Packet Radio Link Layer Protocol
CALL	Call Sign
COTS	Commercial off the shelf
CRC	Cyclic Redundancy Check
EPS	Electrical Power System
FEC	Forward Error Correction
FEM	Finite Element Method
FHWN	Fachhochschule Wiener Neustadt
GFSK	Gaussian Frequency Shift Keying
GNSS	Global navigation satellite system
GPIO	General purpose input/output
GPS	Global Positioning System
GS	Ground Station
I^2C	Inter-Integrated Circuit
ISS	International Space Station
HKD	House Keeping Data
IARU	International Amateur Radio Union
OBC	On Board Computer
LEO	Low Earth Orbit
JTAG	Joint test action group
MCC	Mission Control Center
mNLP	Multiple Needle Langmuir Probe
MPPT	Maximum Power Point Tracker
MRAM	Magnetoresistive random access memory
PID	Protocol Identifier
PPT	Pulsed Plasma Thruster
PSLV	Polar Satellite Launch Vehicle
RSSI	Received Signal Strength Indicator
RX	Receiver, receive
SEL	Single event latch up
SDC	Space Data Center
SPB	Side Panel Bus
SPI	Serial peripheral interface
SSO	Sun Synchronous Orbit
STACIE	Space Telemetry And Command Interface
STG-A	Space Tech Group Austria
TRX	Transceiver
TX	Transmitter, Transmit
TT-64	Thomas Turetschek -64 protocol
TT&C	Telemetry Tracking & Command
TVT	Thermal Vacuum Test
UART	Universal asynchronous receiver transmitter
UHF	Ultra High Frequency

1. INTRODUCTION

QB50 is an international project, which has sent 36 Nanosatellites, a.k.a. CubeSat, into the Thermosphere[1],[2]. The scientific goal of this mission is to monitor the prevailing conditions in this rather unknown part of Earth's atmosphere over a period of up to nine months. Each of the nanosatellites within this project was equipped with one of three possible scientific instruments: (i) a set of Langmuir probes, (ii) atomic oxygen measurement device, (iii) ion/neutral mass spectrometer. Most of the satellite were built by CubeSat teams from all over the world. The satellites were launched in two batches. The first batch of 28 satellites was released from the International Space Station in April 2017. The second batch, including PEGASUS, was launched with the Indian PSLV on the 23rd of June in 2017.

PEGASUS is the very first 2U CubeSat build and launched by Austria. Under the leadership of the University of Applied Sciences (FHWN), PEGASUS was designed, manufactured and qualified by the FHWN and its research company FOTEC, with its partners the Space Team of the Technical University of Vienna, the Space Tech Group Austria (STG-A) and many others.

One of the initial decisions in the PEGASUS project was to design the satellite from scratch instead of relying on procured subsystem. Although this decision caused many delays, at the end, the educational benefit was tremendous and some of the design solutions are unique (see subsystem description in the following). Only two subsystems of PEGASUS were procured, namely the dipole antenna (AntS) from ISIS[3] and a GPS from Skyfox Labs[4]

While the satellites from the first batch had a rather short lifetime of 6-10 months due to the fact that they were launched from the ISS (orbit altitude ~400 km), PEGASUS and the other 7 satellites which were launched in the second batch into a SSO with an orbit altitude of ~500 km have an expected lifetime in orbit of 6-7 years.

In order to ensure the capability to collect and downlink data over several months, PEGASUS requires about the same types of subsystems as one would find on large-scale satellites. This includes an attitude control system, an on-board computer, telecommunication devices, an electrical power system allowing to harvest the solar power and either distribute or store it for later use, a thermal control system – to name only some. In addition to the above, PEGASUS also features a propulsion system which, if successful, would be the first time to use such a system on a nanosatellite.

When writing this paper, PEGASUS has successfully operated for 15 months in orbit. The commissioning of all subsystems took several months due to some anomalies observed in some subsystems and their subsequent analysis and correction. Most of the anomalies have been removed or a work-around them has been implemented. PEGASUS is equipped with the aforementioned Langmuir probes and started four months after the launch to provide information about essential properties of the plasma in the thermosphere such as the electron temperature and –density.

2. PEGASUS DESIGN SUMMARY

As mentioned above, only two satellite subsystems of PEGASUS have been procured. All others were designed by the PEGASUS team. Beside of the science unit (multi needle Langmuire probe), PEGASUS has the usual subsystems on board, namely an on-board computer (OBC), an UHF transceiver and two dipole antennas, an electrical power system consisting of a power processing unit, 16 triple junction solar cells (two solar cells always in parallel in combination with a MPPT), and a GPS with a batch antenna. In addition to those systems, PEGASUS also carries a miniaturized Pulsed Plasma Thruster (PPT) on board as a technology verification payload.

The following picture show the internal components of PEGASUS as well as a view of the outside of the satellite (identical on all sides)

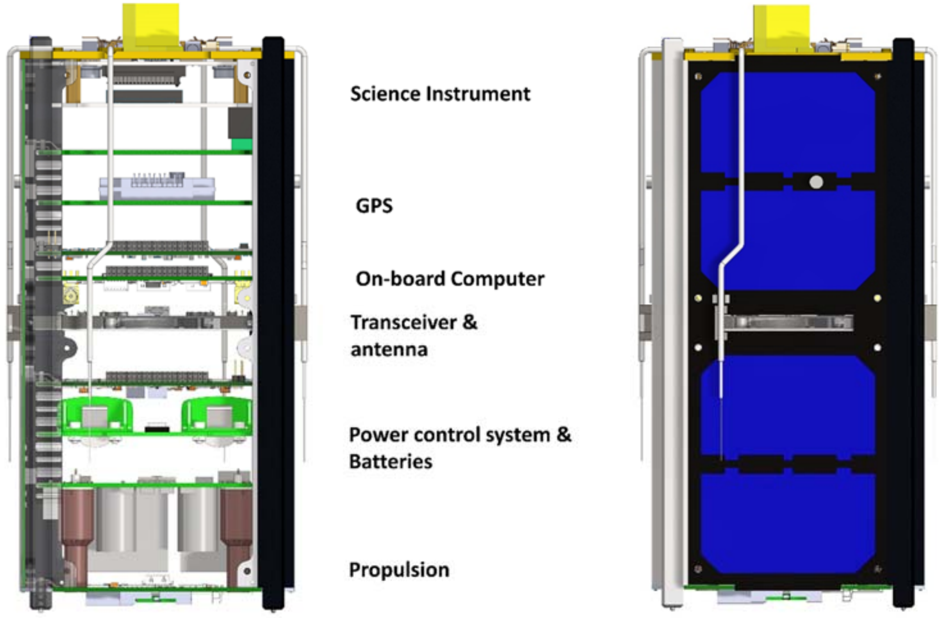

Figure 1: Design of PEGASUS with its internal components (left) and a view of the outside (right)

2.1 Structure and thermal control system

The PEGASUS team decided early in the design process not to rely on commercially available systems as much as possible. This included also the satellite structure for which the team developed their own solution. This decision freed the team from constrains deriving from limitations due to the nature of how subsystems are mechanically and electrically integrated into the structure. In particular important was the removal of the PC104 connector widely used in the community but considered by the team as an inefficient use of volume and mass. Furthermore, it allowed the team to implement and test some innovative ideas. As described in the following, parts of the developed structure are multifunctional insofar that beside of being a part of the structure they are also essential part of the EPS and ADCS.

The PEGASUS structure consists of four rails (AL6061) located at the four concerns of the satellite (see Figure 1) and four side panels, as well as a bottom and a top panel. All the panels are bolted to the rails and together they are the sole elements of the structure. In addition to be part of the structure, the panels have multiple other functions. Basically they are printed circuit boards (PCB) serving also as backplane connector. All PEGASUS subsystems are mechanically fixed to the rails and use one or several of the side panel to connect electrically with other subsystems. This had the effect that PEGASUS hardly needs any cables (with the exception of the kill switches and the high frequency cable for the communication and GPS), which simplified assembly significantly. Furthermore, each side panel contains a magnetotoquer, interfaces for a photodiode (both for ADCS purposes) and provides the mechanical, thermal and electrical interface for the solar cells.

The development of the structure was guided by FEM analysis and, in parallel, several vibration test were conducted to verify the numerical results and the proper design (see Figure 2).

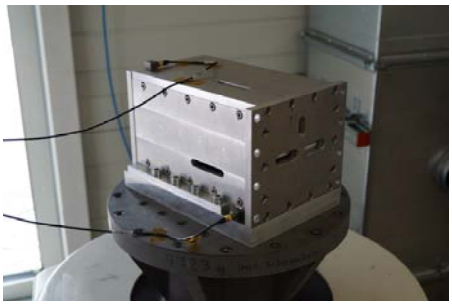

Figure 2: PEGASUS inside the test pod assembled on the FOTEC vibration table

The thermal environment in LEO is rather modest and not much effort was invested into the development of a thermal system. The satellites surface (panels as well as rails) were colored black to limit radiation losses and the two batteries were equipped with individual heaters (simple heating wires wrapped around the batteries). Simulations showed surface temperatures between +51°C (worst hot case) and -35°C (worst cold case, i.e. no internal heat sources).

Figure 3: PEGASUS EM during TVT (FHWN/FOTEC test chamber)

Several thermal vacuum tests were conducted in order to verify operation (especially for the hot case), proper function of the deployments (burn wires) and battery heaters also at extreme cold temperatures. For such tests, an improvised TVT chamber was utilized which consisted of a bell jar located inside a thermal rack. The set-up (without the bell jar) is shown in Figure 3. Qualification testing was done in an industrial TVT chamber with the kind support of RUAG GmbH.

2.2 Communication

2.2.1 Space segment

STACIE-Δ (Space Telemetry And Command Interface) is an in-house development of the TT&C communication interface. Receiving and transmitting are both done in the 70cm amateur radio band using the time division multiplex method (semi duplex communication). This TT&C interface provides two redundant transceivers with corresponding controllers located on a single board. STACIE-Δ can be powered by two independent power supplies (for each transceiver-controller). Both transceiver-controllers can be operated independently in the same or different frequencies, with the same or different RX or TX frequencies. Frequency-hopping is also possible as diversity RX. All frequencies can be changed remotely from the ground station. A data and control connection between the two TRX controllers decide every time the best RX or TX possibilities. In case of a malfunction of one channel, the other channel takes over the operation and acts as a single TT&C. The encoding and decoding of the data is done by STACIE-Δ similar as the FEC (Reed Solomon) and CRC calculations. Furthermore the controller capabilities of STACIE-Δ are powerful enough to deploy antennas in an automatic deploy process, depending on the availability of electrical power of the satellite. Collecting telemetry data from the EPS over the I^2C bus and transmit beacons independently of the OBC is a further feature. Table 3.2.1 shows the technical specifications of STACIE-Δ.

Table 1: Technical specifications of STACIE-Δ

Frequency range:	413- 453 MHz
Temp. range	-40 - +85°C
Output power max	30dBm, 1W
VCC	3 – 5,6V
Power consumption TX	2,75W @30dBm
Modulation	GFSK
Data rate downlink	9,6k – 256k
Data rate uplink	123 – 9.6k
Data Bus	2x I^2C, 2x UART, 2xGPIO
Sat System Bus	Side Panel Bus (SPB)
Protocol	TT-64
Communication method	Time division multiplex

A command-set, which exclusively acts to the communication interface, allows changing various parameters such as RX frequency, TX frequency, TX power, beacon duration, operation mode and the reset of the OBC. The antenna, an ISIS AntS, in the 2-UHF-dipole configuration, is powered too by STACIE-Δ during deployment and operation over the AntS-SBI (System Bus Interface).

2.2.2 Ground segment

A small ground station (GS) network consisting of 4 GS distributed all over Austria was established. Figure 4 shows the block diagram of the ground segment. The GS are connecting with the SDC (Space Data Center) over the Ethernet. The SDC is managing the GS, requests status reports, is transmitting commands over the GS and gives information about the next satellite transit to the GS.. The GS transmits the collected data to the SDC where the data is analysed and stored in a database. The clients, building the MCC, are connected over the Ethernet to the SDC, where the operators are authenticated and will get the, for the operation of the satellite necessary data, visualized depending on the authentication policy. The transceiver and antenna rotating controller of the GS, STACIE-Γ, is an in-house development. STACIE-Γ consists of a half STACIE-Δ, connected to a Raspberry PI. While STACIE-Γ acts as the TRX module, the Raspberry Pi is the gate to the SDC and the controller of the satellite antenna rotator.

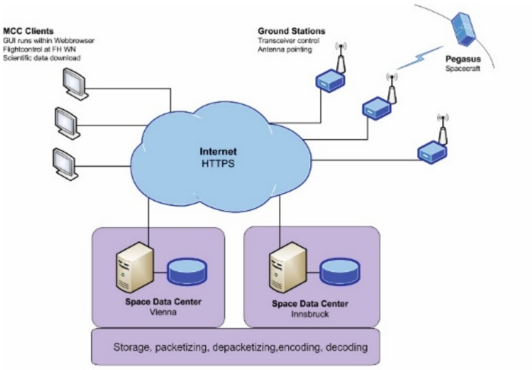

Figure 4: Block diagram of the ground segment

All GS of the GS network are located in Austria, one in Langenlebarn (Lower Austria) one in Wr. Neustadt (Lower Austria), one in Mäder (Vorarlberg) and one, which is an omnidirectional, in Vienna. The SDC is located in Vienna (main and mirror at two different companies, which offer commercial server services).

2.3 On-board computer

The on-board computer (OBC) is the core management system of PEGASUS. It provides communication to and control of all subsystems of the satellite. A NXP LPC1769 is used as main controller, which is a commercial off-the-shelf (COTS) component. This controller is equipped with 512 kB of internal flash and 64 kB of RAM, as well as a variety of interfaces, such as UART, SPI, I2C and JTAG. An integrated real-time clock module (RTC) with independent, buffered supply enables permanent availability of mission time and date, regularly synchronized to the GPS time. An array of three EEPROMs (8 KB, 24AA64T) is utilized to store status and housekeeping information, commands and flash pointers. Triple modular redundancy with automated error repair is implemented in software to ensure reliable storage of this data. Additionally, two redundant flash memories (128 MB, S70FL01GS) are used for mission and measurement data storage. Furthermore, a second micro-controller from Texas Instruments (MSP430FR5728, limited radiation tolerant), supervises the main controller and therefore acts as external watchdog. The OBC provides several measurement values, such as temperature (TMP100), magnetic field (HMC5883, MPU9250), angular rate (MPU9250, LPY403AL, LPR403AL). The algorithm of the attitude determination and control system (ADCS) is executed by the OBC using the internal sensor values, as well as measurement values from external subsystems (GPS, sun sensors, magnetometers). Independent latch up protection switches for the main controller, as well as the second micro-controller and automatic selection and switchover of two 3.3 V power rails, ensure stable and save environment for the OBC. All inputs and outputs of the OBC are equipped with overvoltage, overcurrent and ESD protection. Power supply of many external subsystems is managed by the OBC, which also has the possibility of disconnecting subsystems from the communication busses (I2C). Figure 5 shows the flight hardware of the OBC.

2.4 OBC software

The OBC software is designed in a layered approach. Each layer has a dedicated interface to its upper and lower neighbors, and these interfaces are designed for testability. Each layer can be tested using a dedicated test bench to ensure proper operation before they are combined to the whole system. Figure 3.2 shows the layered architecture of the Pegasus software system. The first layer (Interfaces) consists of device drivers for the periphery of the OBC as well as the other subsystems of PEGASUS. It provides low-level functions to establish communication via various interfaces such as SPI, UART and I2C.

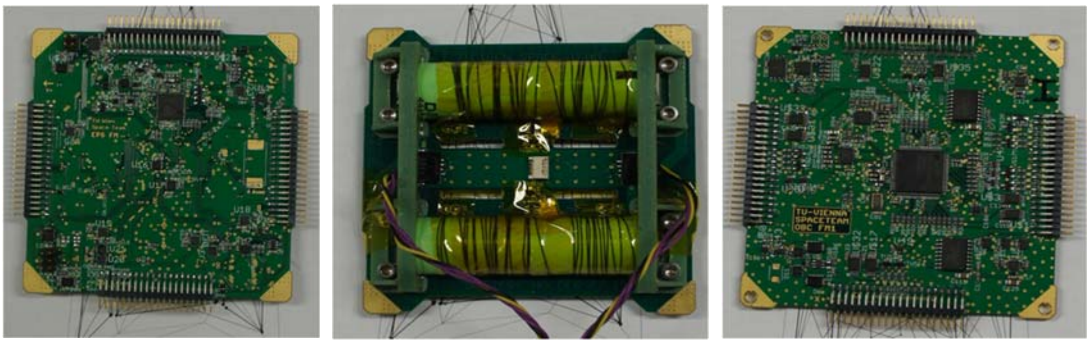

Figure 5: PEGASUS EPS (left), Battery unit before installation of multilayer insulation (middle) and OBC (right) from Space Team, TU Vienna

Layer two implements periodic readout from all sensors and subsystems of PEGASUS. Acquired values are checked for plausibility, checksums are verified and their quality is rated. If necessary filtering is applied. The status of each software/hardware interface is monitored permanently and re-initialization procedures are executed automatically.

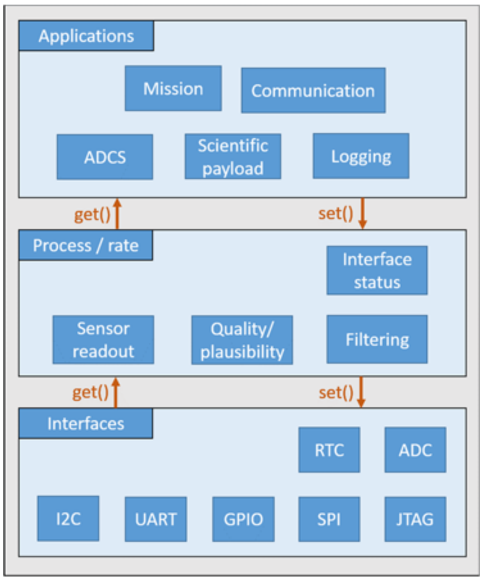

Figure 6: layered architecture of the Pegasus software system

The top layer is the application layer. Besides mission specific tasks such as mission planning and task/command execution, high-level communication to/from the ground station is established. The ADCS algorithm as well as the logging module (high-level data storage and readout) are considered as own applications. If advised by the mission application, the scientific payload application enables communication, control and supervision of the scientific payload. Measurement Data including housekeeping status and error protocols retrieved by the scientific payload are enriched with timestamps and positional data from ADCS. These records are persisted by logging module, which also controls the first-in-first-out queues used for later downlink data communications.

2.5 Electrical Power System

The Electrical Power System (EPS) is designed with a high level of redundancy in mind. The energy from the solar cells is transmitted over two separated power busses and stored in two separate batteries. The EPS can generate two independent regulated output voltages, 3.3V and 5V, using efficient buck-boost switching converters of type LTC3785. The switching converters can be connected to either one of the two power busses. The 3.3V supply for the OBC can also be provided by an additional linear voltage regulator. The linear regulator is supplied either by the solar power busses or directly from the batteries, thereby bypassing a number of critical components. Three independent microcontrollers of type Atmega128 (Atmel), Attiny1634 (Atmel) and MSP430FR (Texas Instruments) are used to control the function of the EPS. Two of these microcontrollers function as dedicated communication controller, handling the communication to the OBC. The third microcontroller controls the overall function and data collection of the EPS. The two communication controller are additionally used as backup for the main controller, by allowing them access to some critical components, such as the linear regulator or the main battery switches. Besides the two independent communication busses to the OBC, the EPS is also directly connected to the TT&C via an I^2C bus, serving as a backup communication line. Figure 5 shows the flight hardware of EPS and battery holder.

2.6 Attitude Determination and Control System

The QB50 project had only two dedicated ADCS requirements: (1) the attitude control shall have a pointing accuracy of 15° with a pointing knowledge of 5° and (2) the CubeSat shall be able to recover from tip-off rates of up to 50 °/s within 3 days under nominal conditions. Initial assessments showed that compliance with those requirements can be achieved solely through the use of magnetotorquers, allowing the avoidance of mechanically more complex reaction wheels. The coils for the magnetotoquers were integrated into the side panels (the outer layer clearly visible in Figure 8, top). The side panels are PCBs with four 70µm copper layers. Three layers of each side panel contain windings of one single coil resulting in 0.64 m² effective area, such that PEGASUS had two opposing coils to produce a magnetic dipole in x direction and two in y direction. For x and y direction, a magnetic moment of 0.21 Am^2 is therefore generated. The magnetic moment around the z axis was generated with a dedicated PCB inside PEGASUS. Due to its limited size, the z axis magnetic moment was only about 1/3 of the magnitude in x and y direction. Simulations show clearly that this magnetotorquer configuration was compliant with the QB50 requirements (see Figure 7). Since only the magnetorquers are used to detumble the spacecraft, the angle between the magnetic field vector and the required torque to spin down is important. At 90° detumbling is most efficient – between 60° and 120° detumbling is active. Outside this range, the spacecraft would spin up around another axis, which is to be avoided.

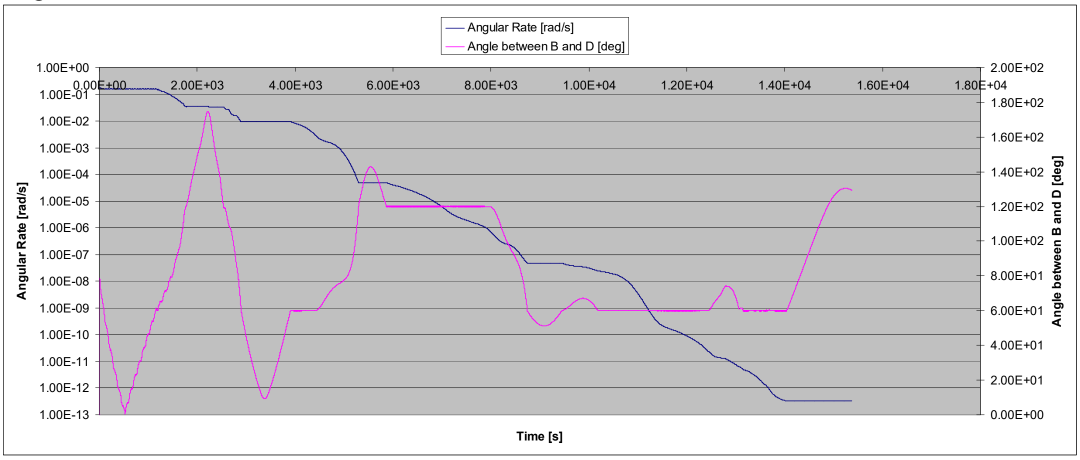

Figure 7: Detumbling simulation of PEGASUS. Angular rate (blue) and angle between magnetic field and required torque axis (violet).

There are different means to determine the spin rate of the spacecraft. Depending on the spin rate of the spacecraft, different means are used to accurately determine the value.

- Coarse gyroscope type ST L3G4200D: this gyroscope is used to measure high spin rates (up to 2000 deg/s)
- Fine gyroscope of type LPR403AL and LPY403AL: at lower spin rates this device offers improved accuracy due to a lower static offset
- Derivative of the orientation matrix: at very slow spin rates (~ minutes per rotation), the spin rate is computed from the change of the orientation matrix.

The Pulsed Plasma Thruster (PPT) can also be used to control the satellites attitude around 2 axes. However, the PPT was a technology demonstration to be used following successful science operation and it was not planned to use it for ADCS purposes in nominal operation. PEGASUS had three different sensors on board aiding the ADCS. A magnetometer is sitting on a nine cm long deployable boom (the white boom shown in Figure 8, bottom) and a visible light photodiode, TEMD6200FX01, is attached on each of the six panels (see also Figure 8, top). The photodiodes were calibrated with a solar simulators and the measurement was temperature compensated.

2.7 Pulsed Plasma Thruster

Pulsed Plasma Thrusters (PPT) have a very simple mechanical design (allowing straightforward miniaturization), and have a very low power demand. Both are features, which make them very attractive for CubeSats. An additional system benefit of PPTs is the quasi-neutrality of the expelled plasma, making any charge neutralization means, usually required for ion thrusters, obsolete. In contrast to other EP thrusters, comparatively low voltages are required to operate the PPT, which increases the reliability and protection of the entire spacecraft as well.

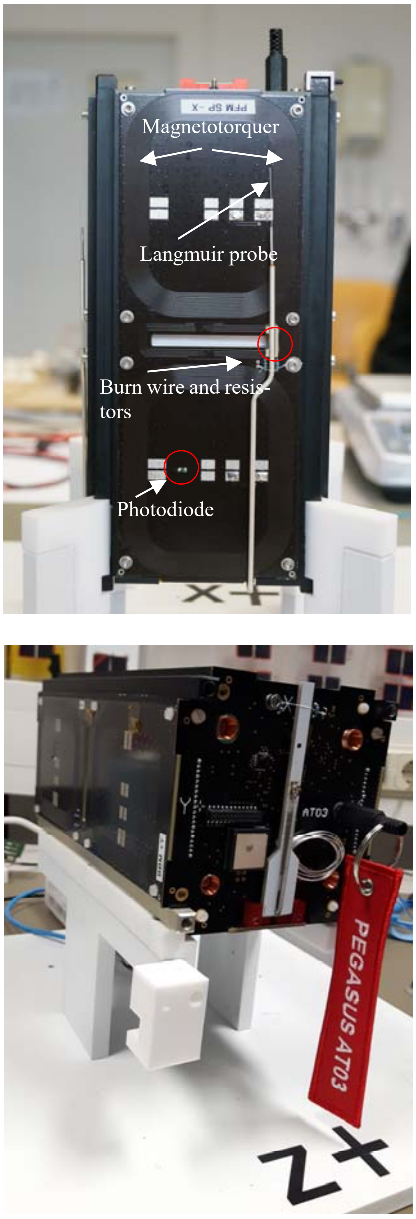

Figure 8: Side panel of PEGASUS showing several features (left) and the Z+ side of the satellite showing the boom (white) with the magnetometer as well as the four PPTs (right picture)

The PPT utilized for PEGASUS has a coaxial geometry, offering favorable mechanical and physical properties. The outer electrode (hollow copper cylinder) fully confines the propellant and the plasma during ignition and acts as a shielding barrier protecting the surrounding structure. It is therefore not required to utilize additional means against strong electromagnetic induction or carbon deposition. The PPT system for PEGASUS features four thruster heads sharing common power and control electronics. Some of the key features of the propulsion module are as follows:

- Generation of 1.35 kV at 1.8 mA (energy storage)
- Generation of 400 V at 1 mA (ignition)
- Four independent ignition circuits
- Feedback signal indicating successful ignition
- Digital control and interface to onboard computer

The Propulsion system uses highly efficient and lightweight DC/DC converters which transform the spacecraft bus voltage of 5 V to up to 1350 V. The propulsion system is equipped with digital TTL I/O lines, which can be connected to any onboard computer. An enable line is utilized to power the whole system. Four ignition lines are used to ignite one of the four thrusters. A feedback line, which is controlled by the propulsion system, is pulled to logic high when a successful ignition has occurred.

Each thruster head can produce a thrust of 2.2µN at a specific impulse of 600 s. Ground showed a lifetime of at least 700,000 discharges producing a total of 5.7 Ns and a total dv for the 2U PEGASUS of 6 m/s.

3. SCIENCE OBJECTIVE AND INSTRUMENT

Essentially all our knowledge about ionospheric plasma density structures with scale sizes of a few tens to hundreds of meters was derived from indirect measurements. It was shown, for example, that electromagnetic signals received on the ground frequently contains fluctuations in amplitude and phase, so-called scintillations[5]. These are imposed on the signal as the wave travels through an ionosphere that contained plasma density irregularities. These irregularities would locally alter the refractive index and therefore cause minute differences in the travel time for selected parts of the wave front, combining to cause sometimes significant signal distortions. Radio communication and Global Navigation Satellite Systems (GNSS) both suffer from ionospheric scintillations, and the problems are most severe at low and high latitudes[6,7]. The Pegasus satellite orbits Earth in a polar orbit, which would offer a good opportunity to revisit instability regions in the thermosphere at approximately 500 km altitude and to study growth and decay of the instability regions.

Langmuir probes have been widely used as diagnostic instruments for both laboratory and space plasma[8,9]. The instrument operation normally consists of sweeping the probe through a range of voltages from negative to positive. Sweeping will produce a current-voltage characteristic curve, from which plasma parameters such as electron density, electron temperature and plasma potential can be determined[10]. However, sweeping takes time on order of 100 ms and makes this approach unsuited for high spatial resolution measurements to study plasma structures with LEO satellites. The multi-needle Langmuir (m-NLP) science unit on board Pegasus has been built at the University of Oslo (UiO)[11]. The m-NLP instrument designed for the QB50 mission is capable of measuring electron density with a temporal frequency of up to 255 Hz. It accomplishes this by having four cylindrical Langmuir probes (so-called needles with diameter of 0.29 mm and length of 25 mm) biased at different voltages within the electron saturation region such that the currents to these four probes can be sampled at high rates. The electron saturation current of a cylindrical probe with a radius much smaller than the Debye shielding distance is in the orbital-motion-limited (OML) theory given as:

$$I_c = N_e A e \frac{2}{\sqrt{\pi}} \sqrt{\frac{k_B T_e}{2\pi m_e}} \sqrt{1 + \frac{eV}{k_B T_e}} \qquad (1)$$

where N_e is the electron density, k_B is the Boltzmann constant, T_e is the electron temperature, e is the electron charge, A is the probe surface area, m_e is the electron mass and V is the probe bias potential with respect to the plasma potential, $V = V_b - V_p$. The m-NLP method[12,13,14,15] of determining electron density then requires the difference in the square of collected currents ΔI_c^2, and the difference in the probe biases ΔV_b;

$$N_e = \frac{1}{KA} \sqrt{\frac{\Delta I_c^2}{\Delta V_b}} \qquad (2)$$

where $K = \frac{e^{3/2}}{\pi} \sqrt{\frac{2}{m_e}}$ is now a constant factor based on the electron charge and mass. In addition to the Langmuir probes, the m-NLP science unit also includes an electron emitter to alleviate spacecraft charging effects on the small spacecraft platform. Further detail about the electron emitter can be found in Hoang et al.[15]. The m-NLP system on board Pegasus can help to explore temporal evolution of F-region plasma irregularities in the polar caps, hence be valuable to any attempts to regional or global forecast services.

4. IN-ORBIT RESULTS

The following chapters provide an overview of the operation and performance of some of the subsystems of PEGASUS but not all of them. It has turned out that the data rate of some measurements is just not sufficient to assess certain situations. If a temperature is measured with 1Hz this is in general sufficient. However, if a gyroscope or the photodiode provides data with a 1 Hz rate, it is very often difficult or impossible to get a meaningful result. In addition, no data can be provided from the Pulsed Plasma Propulsion at this point due to software issues.

4.1 Launch, commissioning and operation

PEGASUS was launched on June 23rd, 2017 by the Indian launcher PSLV from the Satish Dhawan Space Centre in India at 03:59 UTC. Together with the major payload, the Cartosat 2E earth imaging satellite, PEGASUS and 30 other CubeSats were injected into a Sun Synchronous Orbit (SSO) at 510 km altitude. Several hours later, the PEGASUS ground stations received the first beacon signals. In the first beacons, the battery voltage of one battery showed extremely low voltages indicating a completely discharged battery (only some weeks later after a detailed error analysis, it became clear that the batteries were not discharged, rather the OBC needed a reset to reinitialize the sensor interfaces).

Since at this early point in time during the mission the above mentioned error was not understood and since all other systems seemed to operate nominal, the decision was taken to not initiate the commissioning phase directly after der launch but rather allow the batteries to warm up and recharge. During this time several tests were performed and measurement values of all sensors were verified to be sure, the satellite works as designed.

Data provided by the Joint Space Operation Center (JSpOc) with regard to collision warnings, so called Conjunction Data Messages (CDM), are collected and used for the following analysis. During the first year of PEGASUS in orbit, a total of 711 conjunction warnings with 70 different objects were issued (see Figure 9). Of those conjunction warnings, 20% were triggered by objects classified as debris, including objects such as the infamous Fengyun 1D but also by upper launcher stages as well as by satellites such as the inactive Japanese satellite ASTRO H. 35% of the warnings were triggered by satellites launched together with PEGASUS on the PSLV launcher. 21% were triggered by objects not on a SSO, the largest part of those (71%) by satellite (or satellite debris) from the Cosmos series.

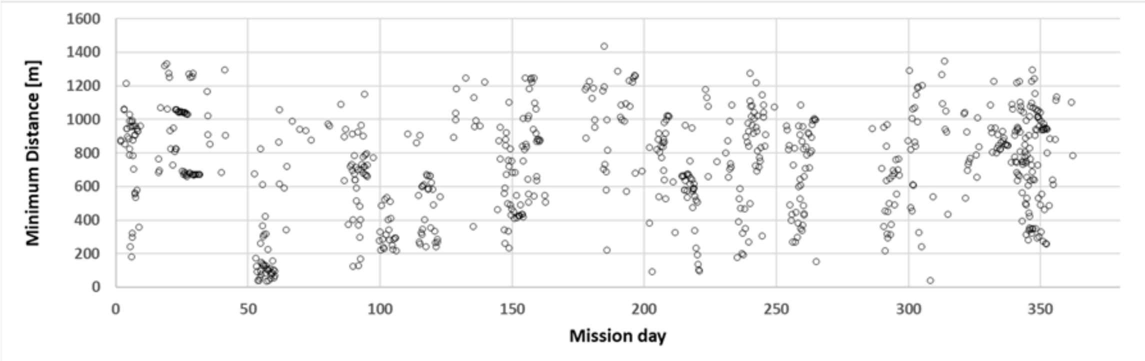

Figure 9: An overview of all CDMs during the first year of PEGASUS in orbit

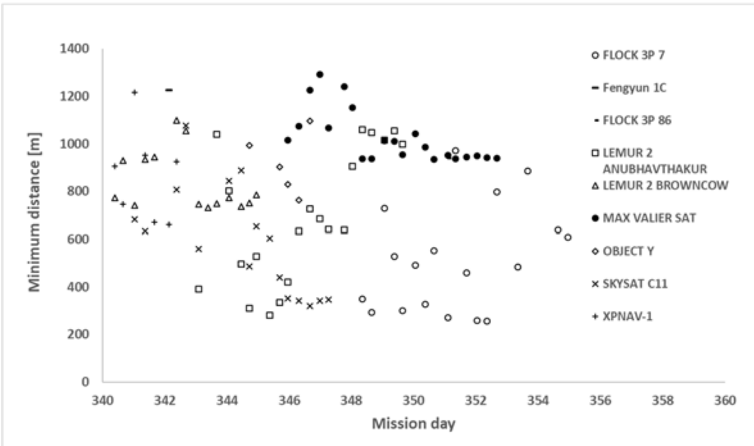

Figure 10: A zoom into Figure 9 showing the CDMs during a two period week featuring the highest rate of CDM during a two-week period encountered during the time of PEGASUS in orbit

Two periods during those 360 days are of special interest. Around day 55, an accumulation of collision warnings with very low minimum distance was issued. The lowest minimum distance was 34 m. All of those warnings were due to Diamond Green, one of the three 3U CubeSats launched by the UK consortium SSG on the same launch as PEGASUS. For a period of about 8 days, Diamond Green and PEGASUS were very close together and more than 40 collision warnings were issued before the two satellites drifted apart again. The second period of interest is at the very end of the first year in orbit. The frequency of warnings increased significantly for two weeks following day 340. A detailed assessment of the period is shown in Figure 10. In those 14 days, nearly 100 collision warnings were issued, 70 of those with satellites, which are part from larger formations (Planet, Spire). Only 20 CDMs were issued due to Max Valier Sat, which was launched together with PEGASUS.

While the above summary of the CDMs seems in the first instance scary for any spacecraft operators, one has to understand that the probability of a collision is in the most case given as zero. Even in the cases where the minimum distance is around 300 m, the probability of a collision is given with $<10^{-6}$.

4.2 Langmuir Probe performance and results

Figure 11 shows the measurement data obtained on February 18th, 2018. The m-NLP probes were biased at 2.5 V, 4.0 V, 5.5 V and 7.0 V. Several anomalies, e.g. the current from the 2.5 V probe is higher than that from the 4.0 V probe for most of the measurement time, are observed from the Figure 11. Since the satellite attitude data are not available yet, it is difficult to understand what happened to the m-NLP probes. For the sake of estimate roughly the ambient plasma density, data from probe 4 (CH4) is used to calculate, which is inferred from an approximation of the Eq. 1 for a single probe with high bias. The electron emitter filament voltage was at 1.14 V during this measurement process. The estimated electron density varied from 1.5 – 2.5 × 10^{11} m^{-3} is shown in the middle panel of Figure 11 together with the electron density derived by the International Reference Ionosphere (IRI-2016) model. The IRI model is an empirical model providing estimates of ionospheric parameters from an altitude of 50 to 2000 km[16]. It can be seen that, the electron density calculations of the two approaches appear to be more or less in the same range. The satellite location and altitude above WGS84 are shown in the bottom panel of the Figure 11.

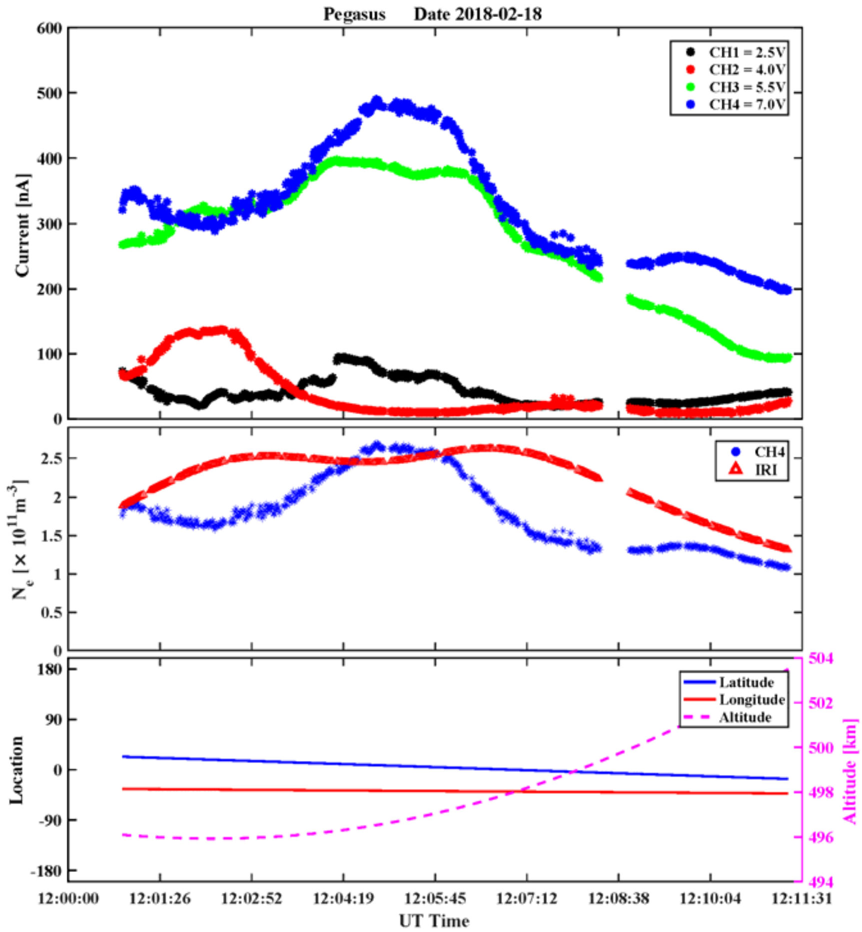

Figure 11: Measurement data from the m-NLP instrument on February 18th, 2018. Top panel shows the currents collected by the four probes. Middle panel shows the comparison between the electron density estimated by the 7.0 V probe and that estimated by the IRI model. The bottom panels shows satellite location (left axis) and altitude above WGS84 (right axis).

4.3 Power harvesting and EPS operation

Temperature characteristics of the power supply system

The EPS and battery pack were designed and tested for an expected temperature range of -20°C up to 60°C. As such, only industrial or automotive grade components were used with temperature capabilities that well exceed the required range. The battery pack was designed with additional heater and protective heat shielding to avoid excessive temperature fluctuations of the used batteries. However, after final assembly, the battery heaters malfunctioned and the CubeSat was launched without this capability. The EPS is programmed to protect the batteries from damage due to thermal conditions. The EPS differentiates between discharging and charging of the batteries. Discharging is allowed below 60°C down to -20°C, while charging is only allowed between 55°C down to 0°C. This behavior allowed PEGASUS to operate continuously even without functional battery heaters. The initial commissioning phase confirmed that the actual temperature range, given in Figure 12 for four exemplary orbits, was well within the expected range. Over the course of more than one year of in-orbit operations, the EPS temperature varied within a range of -18°C to 32°C with a mean value of 4°C while the batteries were within a range of -10°C to 26°C with a mean value of 6°C (exemplary samples shown in Figure 13.

Power harvesting and storage
The CubeSat is powered by four solar cells per panel and stores excess power in two 2.25Ah Li-Ion batteries. The typical charging characteristics of the batteries is depicted in Figure 14 over six orbits. The output voltage level during the constant voltage phase of the charging cycle was set to 4.13V, which is below the maximum cell voltage of 4.2V and below the safety level of 4.18V implemented in the EPS, which protects the batteries from overcharging. However, due to unknown reasons, the in-orbit voltage level of the chargers appears to be above 4.3V, which would result in an overcharging of the batteries and triggers the safety system of the EPS when the batteries approach full capacity. With a power budget that is well in the positive range, PEGASUS normally operates with full batteries. This leads to a behavior where the batteries are disconnected from the power bus shortly after the satellite enters the illuminated part of its orbit as the batteries are quickly recharged to the safety level of the EPS. The batteries are then reconnected to the power bus once the satellite enters the shadow of the earth. During this transition, short power outages of the provided output voltages can occur. In contrast, the reset counter of the three microcontrollers on the EPS have so far not incremented, indicating an over one year long, continuous operation of the EPS.

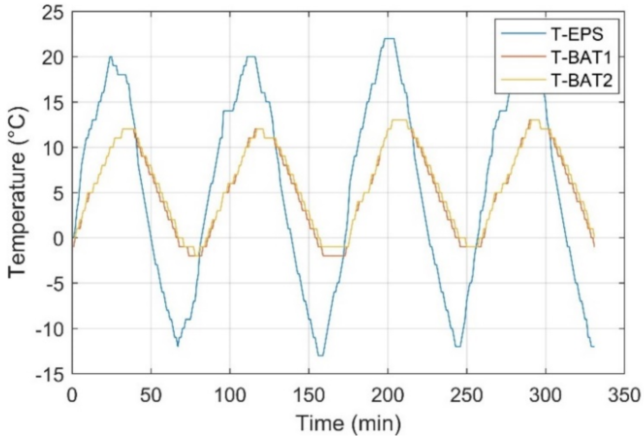

Figure 12: Typical temperature variation of the power supply system (EPS) and the two batteries over the course of four exemplary orbits. Over the course of more than one year in-orbit operations, the temperature of the EPS varied within a range of -18°C to 32°C with a mean value of 4°C. The batteries, which are thermally isolated, varied within a range of -10°C to 26°C with a mean value of 6°C

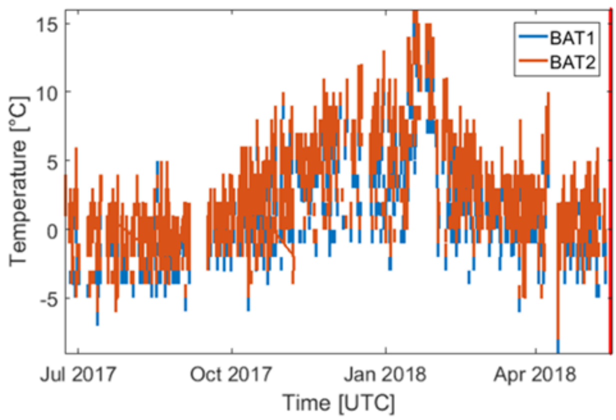

Figure 13: The long term temperature trend of battery 1 and 2, shows an average temperature increase from October 2017 until February 2018. From February until March 2018 the average temperature decreases again to an average around 0°C. This variation correlates with the usage of the science module, where the overall power consumption of PEGASUS was higher.

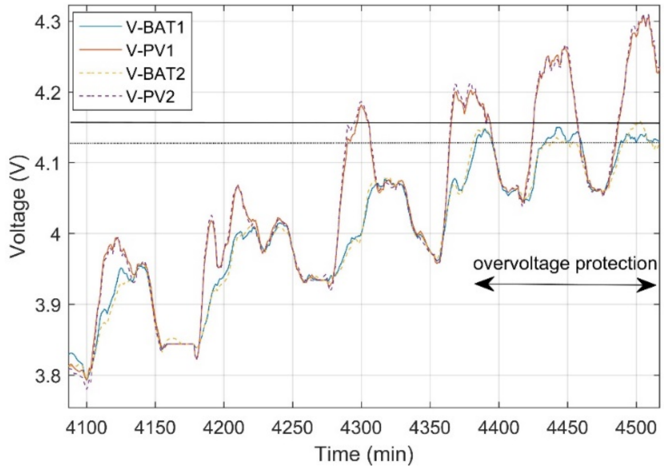

Figure 14: Typical charging cycle of the batteries over five orbits (filtered data). Once the battery limit is reached (solid line), the EPS disconnects the batteries from the solar bus to protect them from overvoltage. The in-orbit charging voltage turned out to be 4.3V instead of the desired 4.13V (dotted line), which cases this unwanted behavior

4.4 Communication

The PEGASUS mission was a test bed for some new concepts in the communication strategy of a CubeSat including a redundancy concept, the implementation of a secondary frequency and implementation of an advanced protocol. Those enhancements are based on some negative experiences of former CubeSat missions of other groups. The idea of absolute communication at any time is a critical issue at space missions.

Redundancy concept:
Redundancy, i.e. the concept of the double TT&C subsystem on one board with the 2 independent 90° crossed dipoles was not only the redundancy in case of a black-out of one TRX-module but also a better transmitting performance. To act on the assumption of a static or very slow rotating satellite, the two TRX modules compare the quality of the last received command and transmit from that one with the better performance expecting that the position to the GS-antennas of this dipole antenna is more efficient. Therefor the STACIE-Δ software checks the weighing out of different criteria: receiver RSSI, receiving power, electrical power of the two power supplies and temperature of the two TRX modules and choose the best side for transmitting. The theoretical forecast shows a fast and often switching between the two trunks. In reality, the switching between the transmitting modules was very seldom, in the most cases only because of electrical power difficulties. The reason is the very low receiving RSSI at the assigned frequency and the very stable temperature of the two TRX modules. As a result of this, the difference of the received signal quality of the two TRX modules is very low, thus no switching happens. The result of the redundant and diversity RX design shows that the concept is working, but the weighting-software needs an improvement.

Secondary frequency:
Frequency hopping of the satellite receivers was also implemented. In case the communication frequency assigned by the IARU (436.670 MHz) would have been blocked by interference signals the STACIE-Δ receivers are listening for commands for 10 seconds after every 4th transmitted beacon to the secondary frequency (438.100 MHz). Even when this short time period was not easy to strike without having an automatically frequency shift mechanism at the GS, successfully commanding at the secondary frequency was performed. Hereby the possibility is given changing the main receiving frequency in case of interferences in orbit.

Protocol:
The unidirectional concept of the STACIE communication design excludes the use of the AX.25 protocol[17]. Instead, a protocol is used, which is specific to the TRX hardware. The so-called TT-64 protocol consists of packets with a length of 64 bytes, including the protocol identifier, the call-sign, 2 bytes of CRC and 16 bytes of FEC. Picture 5.3.1 shows the TT-64 generic packet. With a FEC of 16 bytes it is possible to repair 8 bit defects per packet. A transaction has to be done in a higher layer, but nearly all commands give a respond in the beacons, which are sent every 30 seconds or between data downloads every 25th packet.

After one year in orbit and more than 500.000 received data-packets the conclusion are:

1. A CRC is important to be sure having a correct packet
2. The used FEC is a good and efficient compromise between overhead and repair capability. More than 70% of corrupted packets could be repaired.
3. A transaction oriented protocol is not necessarily required for a satellite communication
4. The performance is high, when using unidirectional transceiving in combination with the TT-64 protocol.

Access time: The daily mean access time from the GS Langenlebarn to PEGASUS during the first year was 1894s/day, which is about 72% of the maximum communication window, which was theoretically calculated for orbits where PEGASUS was able to communicate. 20% of this time was needed for commanding the satellite. Thus 1516s remained for downloading housekeeping data (HKD) and science data. With a mean download rate of 4kbit/s and an overhead of 39%, used for the transmission protocol TT-64, the remaining maximum raw data download amount was 3,6Mbit/day.

RF performance of the radio link: The transceiver operates within the 70cm Ham Radio band and has 1W transmitting power. The strength of the received signal is measured before a packet is sent from ground (idle RSSI) and during an uplink transmission (RX RSSI) Therefore the idle RSSI can be considered as noise background. On the ground station a 40W transmitter is used feeding into 2 stacked X quad antennas with 14.95 dBi gain each. In the receive path a LNA with 20dB gain is used.

The following chart (Figure 16) shows 11000 single measurements taken randomly over a period of one year when the satellite was above the horizon of the ground station.

On average the background noise is -115dBm and the signal strength is -95dBm. This gives a signal to noise ratio in the uplink of **20dB.** The ground station receives the satellite with -90.5 dBm on average.

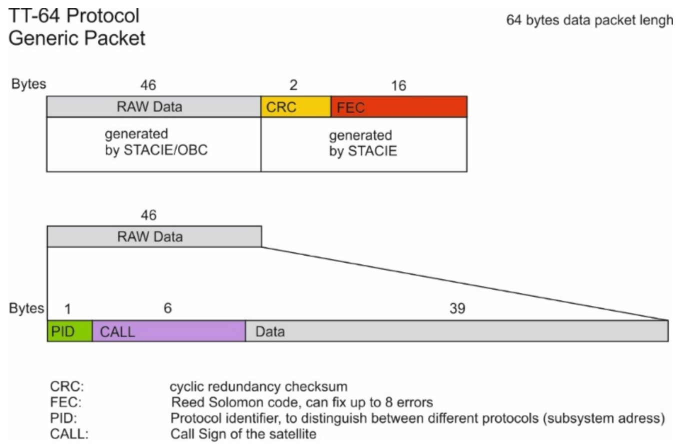

Figure 15: TT-64 protocol, generic packet

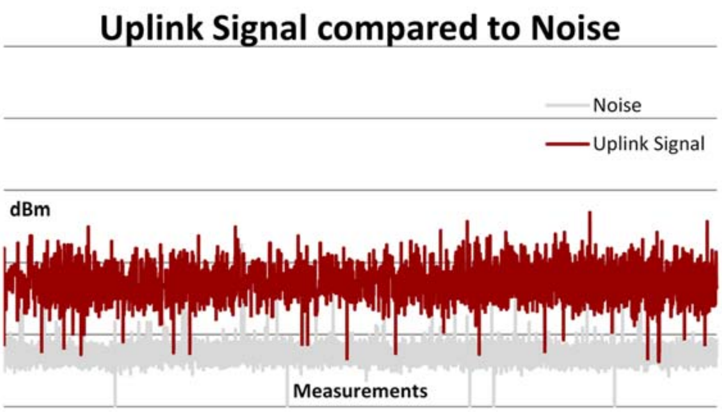

Figure 16: Uplink signal compared to noise

4.5 OBC

The OBC is based on a COTS microcontroller, specifically the LPC1769. As no radiation data of this or similar controllers was available by the time of design, special precautions were taken to prevent/reduce the impact of single event latch-ups (SEL), as well as strategies to deal with bitflips in the program code of the main controller. Current limiting supply switches with automatic recovery are used to prevent damage by SEL.

The program memory of the main controller is checksum protected. The LPC1769 is equipped with an integrated watchdog, which is used to detect software runaways and undefined states. Additionally, an external controller (MSP430) supervises the LPC1769. This controller also implements a JTAG interface to the main controller and has a backup copy of the main controller's program memory stored in the MRAM based storage. If the main controller fails to feed the MSP430 after several power cycles, it is automatically reprogrammed with the backup copy of the program memory via JTAG. However, up to this day this backup system was not triggered. The checksums protecting the internal program memory of the main controller show no errors in the program code and no errors in the unused (blank) section of the program memory. This supports the usability of the used main controller for orbits similar to PEGASUS.

Resets statistic

The main controller implements a reset counter for the OBC, which includes storage of error codes and other information about the cause of the reset. Figure 18 shows the cumulated number of OBC resets over the mission time (starting 30 minutes after deployment). It is clearly visible, that more than 100 resets occurred during the first hours of operation after deployment. As the charging state of the batteries, as well as the battery temperature was low after deployment, regular operation was only possible in direct sunlight. . When PEGASUS entered earth's shadow and the charging state of the batteries was still low, the main controller was able to continue/power up, but energy-intensive events cause the supply voltage to drop and therefore cause a brown-out triggered reset. The OBC was optimized for a fast boot process, which explains the large number of resets in the first hours of operation. After approximately 12 orbits the batteries were charged sufficiently for continuous operation of PEGASUS, the reset rate of the OBC dropped immediately.

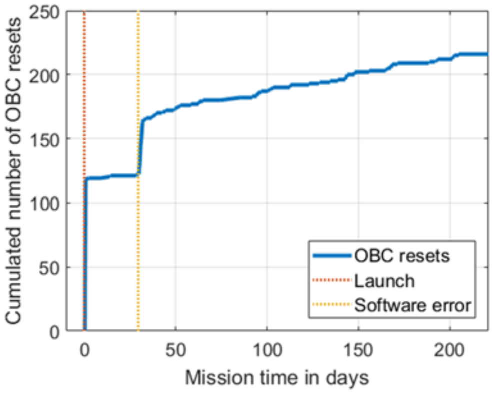

Figure 18: Cumulated resets of the OBC over the mission time. A large number of resets right after deployment due low charging status of the batteries is visible.

From orbit 12 on, the number of resets per time was approximately constant with the exception of a software error at day 30, which generated nearly 40 resets within 3 days. An unexpected character in certain regions of the orbit caused the GNSS parsing algorithm to fail and the main controller to throw a hard-fault condition, which leads to a reset of the OBC.

In Figure 17 the resets caused by these two events have been removed, as their reason is well known. It is clearly visible, that the reset rate of the OBC is approximately constant, which is also indicated by a fit of a first order function to the cumulated resets. In 221 days of operation, which are analyze here, a total number of 56 resets (excluding the previously mentioned resets) was recorded. This results in a reset rate of approximately only one reset in 4 days of operation.

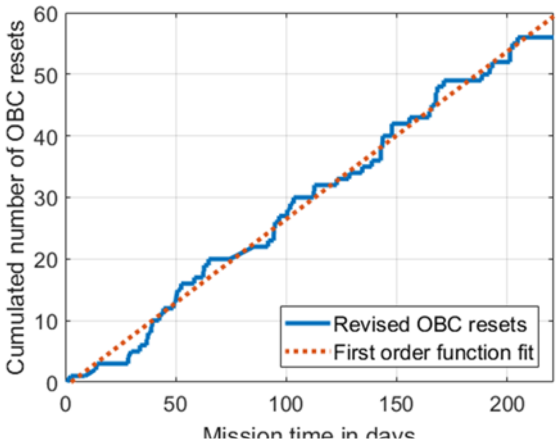

Figure 17: Revised OBC reset number over time. For this plot resets during the first orbits (batteries with very low charging status), resets due to a software error in July and manually triggered resets were removed. On average, one reset occurred in 4 days of operation.

These 56 recorded resets were analyzed to evaluate the performance of the OBC. Figure 20 shows the distribution of events, which caused a reset. The vast majority of resets (38) was triggered manually by the operators of PEGASUS. These resets were used to set the OBC and also attached periphery in a defined state. As the OBC is able to reset attached periphery such as side panel controllers and bottom panel controllers, during its booting process, this option was used to reset periphery controllers, too. Eight resets were caused by the watchdog reacting to the main controller being unresponsive. Four times the OBC was reset due to power supply fluctuations/outages. Six resets could not be specified further in terms of their original cause, as no or only parts of the information necessary was recorded in these cases. Summarizing, less resets due to external events (e.g. radiation, power, aging) than expected were recorded. Excluding manual triggered resets, only 18 event related resets were counted and resolved without any damage by proper implementation of a watchdog, latch-up protection and brown-out supervision.

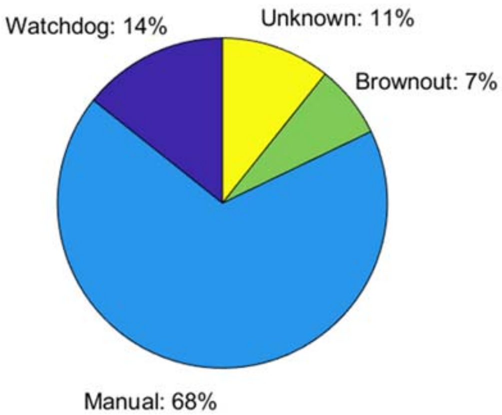

Figure 20: OBC reset reason statistic showing the major amount of resets was intended by mission operators.

Real time clock

The OBC is equipped with a low-power real time clock (RTC) module running on an independent crystal oscillator. During regular operation it is powered by the regulated supply voltage (3.3 V) of the OBC. A capacitor array buffers the RTC for up to 35 minutes, thus ensuring continuous operation even if the regulated supply rail would fail. A direct backup connection to the solar power bus allows charging of the capacitor array without the need of powering the OBC and the EPS.

The RTC time is used as time base for the operation of PEGASUS. Timed execution of commands/tasks is depending on this time, as well as timestamp generation for downlink, logging and

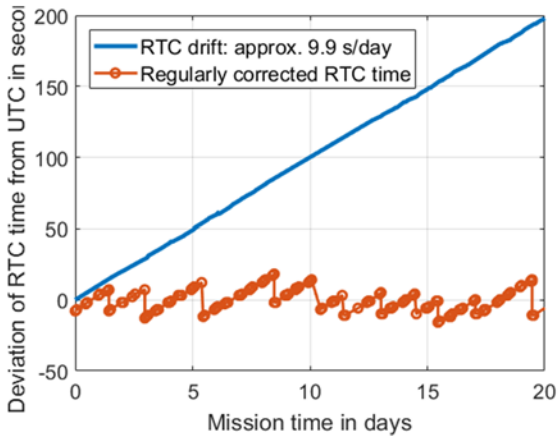

Figure 19: Drift of the OBC's RTC module over mission time. With manual correction the drift is kept in small boundaries around UTC.

the algorithm of the ADCS module. An automatic routine synchronizes the RTC to the time provided by the GNSS module, which is connected via an additional pulse per second output to the OBC.

After the first few days of operation, a comparably large drift of the RTC time to UTC was noticed. *Figure 19* shows the evolution of the time difference between RTC and UTC over mission time. This drift of approximately 9.9 seconds per day stayed constant over mission time. Unfortunately, no possibility to recalibrate the RTC in orbit was implemented. Therefore, the only option was to synchronize the RTC manually (by command from ground station) and by GNSS to keep the time deviation in smaller limits. The result of this (up to daily) routine is shown in Figure 20 in form of a saw tooth signal. With this workaround the RTC time deviation to UTC is kept below 25 seconds.

4.6 Attitude Determination and control

Unfortunately, the ADSC system had several problems. The GPS system worked very well and, following a cold start, a fix was achieved in the matter of minutes. However, every time a fix was obtained, the on-board time of the OBC was reset to 01.01.2000, 00:00. This behavior was not seen at ground tests of the flight unit nor the spare flight unit and is not understood and in spite of excellent support of Skyfox, it could not be solved. This however, resulted in a chaotic mix of old data with new data and in some cases, old data were overwritten by new data with the same (erroneous) time stamp. For those reasons, the operational team made the decision to keep the GPS deactivated for the time being. In addition to the GPS, PEGASUS had some gyros and one photodiode on each side (see chapter 2.6) for attitude monitoring. The data from the gyros drifted strongly and was effectively useless for any analysis. Furthermore, the ADCS algorithm requires a threshold value for the output of the photodiode in order to activate the magnetotorquers for the fine alignment. Below this value, only the de-tumbling mode is activated if the rotation rate exceeds a certain level. Unfortunately, in spite of on-ground calibration of the diodes, in orbit, the value never reached the threshold value. Hypotheses to explain this behavior include an increase in opaqueness due to the rather aggressive atmosphere in this orbit or an erroneous calibration. Fact is, that the rotation was too low to activate the detumbling and the fine-tuning of the alignment was never activated due to the threshold value issue. Manual operation of magnetotorquers was initiated and over several months a change in the rotation rate was observed (Figure 21). However, at this point it is unclear if this decrease in rotation is due to the manual operation or due to natural effects (gravitation alignment etc.). The data depicted in Figure 21, are rotational rates over several months obtained by analyzing the output of the photodiodes. Increasing further the issues PEGASUS had with the photodiodes, the photodiodes on the +Z and +Z sides di not provide any information. Therefore only those data sets where rotation around the z axis dominated were included in the graph show in Figure 21. Keeping this limitations in mind, one can clearly see the above mentioned decrease in rotational speed. However, a clear explanation for this decrease is at the moment hypothetical at best.

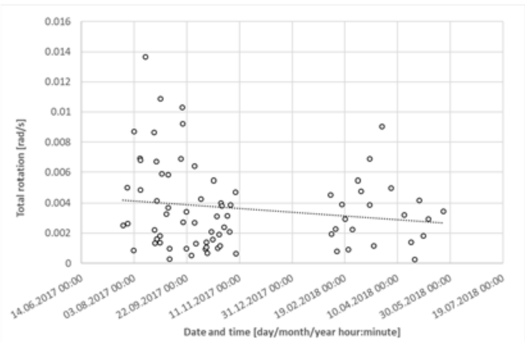

Figure 21: Rotation rate of PEGASUS over several months based on data from the photodiode

5. Conclusions and outlook

The CubeSat PEGASUS was the first Austrian CubeSat build by Students. Following more than 3 years of development and testing, the satellite was launched in June, 2017. Since then it successfully operates in its orbit. About 500,000 data packages have been received since its launch containing a multitude of housekeeping data as well as data from the scientific instrument. While the latter will provide the scientist of the University of Oslo with valuable data for the modelling of the upper atmosphere, the information contained in the housekeeping data is very important to the PEGASUS team. The data allows a better understanding how the subsystems of PEGASUS function in orbit. This again allows the team to improve their systems for upcoming missions. PEGASUs can be considered to be a full success for all participants. The satellite is operating for more than one year successfully in orbit and is still sending data at the point of writing this paper. All the team members have made many important experiences during the project and increased their knowledge tremendously. For all participating students, it was a valuable experience, in-spite, or maybe because of the sometimes stressful and even frustrating process of developing a satellite under the given time constrains and with a minimum of budget. Already now, there is very positive feedback from several students who participated in the PEGASUS project and who are not working in various companies. They express how much this experience helped them for the job application and even in their day-to-day work life. This in itself and the experience to be part in a flight project during their education is probably the most important output a University CubeSat project can have. Most of the new homebrew designs and concepts turned out to be very successful. Nevertheless, improvements are always possible and are already in preparation for the next mission called CLIMB. For example, a complete review of the ADCS sensors and some of the logic behind it, improvement of the RTC stability, more robust software design (to avoid unexpected resets in a more challenging environment) and other improvements.

Acknowledgements

PEGASUS was a part of the QB50 project, which was funded by the European Commission in the FP7 program. The PEGASUS project was internally funded by the state Lower Austria (Niederösterreich), Austria and the University of Applied Science Wiener Neustadt. In addition, many companies or person helped through their expertise, testing facilities or other in-kind contributions. The PEGASUS team likes to express their deep appreciation for this. Without this, PEGASUS would not have been possible, Also, the ministry for transportation provided invaluable help in applying for and receiving the permission for launch. In particular, Mrs. Feige and Mr. Fuchs shall be mentioned here but also the priceless help of Cordula Steinkogler and Professor Marboe of the University Vienna. Both helped to shed some light into the darkness of space law. Many thanks also to Georg Ockermüller from the company GEROCRET for giving the permission to set up a ground station on the premises of GEROCRET.

Many students have worked on the PEGASUS project but are not mentioned in the list of Authors. Nevertheless, without them PEGASUS would not exist. Therefore, many thanks to Daanish Bambery, Masud Feisal, Lionel Gury, David Jelem, Patrick Kappl, Peter Kremsner, Wolfgang Lubowski, Joan Miralles, Varun Nandyala, Prabhat Pant, Christian Plasounig, Mathias Poik, Abouagaga Sameh, Ugljesa Stankovic, Richard Sypniewski, Sencer Yücesan and many others.

[1] https://www.qb50.eu/ , last accessed, April, 2018

[2] Status of the QB50 CubeSat Constellation mission, IAC-14-B4.2.11, 65th International Astronautical Congress, Toronto, Canada.

[3] https://www.isispace.nl/, last accessed, September, 2018

[4] http://www.skyfoxlabs.com, last accessed, April, 2018

[5] J.S. Hey, S.J. Parsons, J.W. Phillips, Fluctuations in cosmic radiation at radio-frequencies. Nature 158, 234 (1946). https://doi.org/10.1038/158234a0

[6] Basu S, Basu S, Equatorial scintillations - a review. Journal of Atmospheric and Terrestrial Physics 43(5), 473 – 489 (1981). https://doi.org/10.1016/0021-9169(81)90110-0

[7] S. Basu, S. Basu, E. MacKenzie, W.R. Coley, J.R. Sharber, W.R. Hoegy, Plasma structuring by the gradient drift instability at high latitudes and comparison with velocity shear driven processes. J. Geophys. Res. Space Phys. 95(A6), 7799–7818 (1990). https://doi.org/10.1029/JA095iA06p07799

[8] R.L. Boggess, L.H. Brace, N.W. Spencer, Langmuir probe measurements in the ionosphere. J. Geophys. Res. 64(10), 1627–1630 (1959). https://doi.org/10.1029/JZ064i010p01627

[9] L.H. Brace, Langmuir probe measurements in the ionosphere. In: Measurement Techniques in Space Plasmas: Particles. Geophysical Monograph Series, vol. 102 (Am. Geophys, Union, Washington, 1998). https://doi.org/10.1029/GM102p0023

[10] F.F. Chen, Electric probes, Academic Press, chap 4, pp 113–200 (1965)

[11] T.A. Bekkeng, E.S. Helgeby, A. Pedersen, E. Trondsen, T. Lindem, J.I. Moen, Multi-needle Langmuir probe system for electron density measurements and active spacecraft potential control on cubesats. IEEE Trans. Aerosp. Electron. Syst. (2017 submitted)

[12] T.A. Bekkeng, K.S. Jacobsen, J.K. Bekkeng, A. Pedersen, T. Lindem, J.P. Lebreton, J.I. Moen, Design of a multi-needle Langmuir probe system. Meas. Sci. Technol. 085, 903 (2010). http://stacks.iop.org/0957-0233/21/i=8/a=085903

[13] K.S. Jacobsen, A. Pedersen, J.I. Moen, T.A. Bekkeng, A new Langmuir probe concept for rapid sampling of space plasma electron density. Meas. Sci. Technol. 21(8), 085902 (2010). https://doi.org/10.1088/0957-0233/21/8/085902

[14] H. Hoang, K. Røed, T.A. Bekkeng, I.J. Moen, L.B.N. Clausen, E. Trondsen, B. Lybekk, H. Strøm, D. M. Bang-Hauge, A. Pedersen, The multi-needle Langmuir probe instrument for QB50 mission: Case studies of Ex-Alta 1 and Hoopoe satellites. Space Science Reviews (2018b submitted).

[15] H. Hoang, L.B.N. Clausen, K. Røed, T.A. Bekkeng, E. Trondsen, B. Lybekk, H. Strøm, D. M. Bang-Hauge, A. Pedersen, A. Spicher, I.J. Moen, The Multi-Needle Langmuir Probe System on Board NorSat-1. Space Science Reviews 214(4) (2018a), https://doi.org/10.1007/s11214-018-0509-2

[16] D. Bilitza, D. Altadill, V. Truhlik, V. Shubin, I. Galkin, B. Reinisch, X. Huang, International reference ionosphere 2016: from ionospheric climate to real-time weather predictions. Space Weather 15(2), 418–429 (2017). https://doi.org/10.1002/2016SW001593

[17] Terry L. Fox, WB4JFI, 1984